2056 © 1982 The Chemical Society of Japan Bull. Chem. Soc. Jpn., 55, 2056—2063 (1982) [Vol. 55, No. 7

Voltammetric Studies of the Use of the Rotated Oxide Electrode as an Indicator Electrode and as a View to the Determination of EDTA and Other Complexanes

Tadayosi Yoshimura

Department of Industrial Chemistry, Fukui Technical College, Sabae, Fukui 916

(Received September 7, 1981)

The accessible potential ranges of rotated lead dioxide (PbO_2) and manganese dioxide (MnO_2) electrodes were investigated in supporting electrolyte solutions of 0.1 mol/l (mol/dm^3) KNO_3 at various pH values, by measuring the base currents of these oxide electrodes. The anodic and cathodic ascending potentials of both the oxide electrodes are pH-independent in a neutral solution. In each neutral system of KNO_3, $KClO_4$, K_2SO_4, and KCl, the accessible potential range of the PbO_2 electrode was from +1.4 to +0.2 V *vs.* SCE, while that of the MnO_2 electrode was from +1.2 to +0.3 V, and the lower manganese oxide electrode from +0.3 to −0.9 V. Furthermore, the applications of these electrodes to the determination of EDTA and other complexanes were examined. Both the oxide electrodes gave a good calibration curve which could establish a linear relationship to the EDTA concentration, passing through the point of origin. The rotated PbO_2 and MnO_2 electrodes seem to be useful for determining depolarizers such as the EDTA-type complxanes.

The voltammetric fundamentals of the oxide electrodes have been reported by several investigators. With regard to the Pt electrode, Kolthoff and Tanaka[1)] reported the residual current-voltage curves and dissolution patterns of rotated and stationary platinum wire electrodes in supporting electrolytes. When the curves are recorded from the evolution potential of oxygen in the negative direction, a small cathodic dissolution pattern is observed starting at a potential which approximately corresponds to the equilibrium value of the platinum-platinous hydroxide electrode. Sato *et al.*[2)] reported the electrodeposition and reduction of the manganese dioxide (MnO_2) electrode; two cathodic waves were observed in an acidic solution in a cathodic sweeping. Similar results were reported by Reynaud,[3)] Lee *et al.*,[4)] and Yoshimura:[5)]

$$MnO_2 + H^+ + e^- \longrightarrow MnOOH, \qquad (1)$$

$$MnOOH + 3H^+ + e^- \longrightarrow Mn^{2+} + 2H_2O. \qquad (2)$$

The lead dioxide (PbO_2) electrode was reviewed by Carr and Hampson.[6)] Under acidic conditions and within the anodic potential range, the primary redox equilibrium is between lead dioxide and the lead(II) ion:

$$PbO_2 + 4H^+ + 2e^- \rightleftharpoons Pb^{2+} + 2H_2O. \qquad (3)$$

The electrode reactions of ethylenediaminetetraacetic acid (EDTA), other polyamine *N*-polycarboxylic acids (complexanes),[7,8)] chromium(III),[9)] acetylacetone,[10)] 8-quinolinol,[11)] and ethanol[12)] have previously been reported by using the stationary MnO_2 and PbO_2 electrodes as indicator electrodes. In the case of the MnO_2 electrode,[7)] a characteristic cathodic peak due to the complex formation of EDTA was observed, and two further anodic peaks or the coalesced anodic peak were at last also observed in an acidic solution. In the case of the PbO_2 electrode,[8)] an anodic peak and a cathodic peak due to the complex formation of EDTA were obtained in a 0.1 mol/l KNO_3 solution. Both the cathodic and anodic peaks of these oxide electrodes increase with the increase in the complexane concentration.

For the analytical use of the PbO_2 and MnO_2 electrodes, it seems to be most useful to investigate and clarify the voltammetric behavior of the rotated oxide electrodes. In this work, the accessible potential ranges of these oxide electrodes were investigated in the supporting electrolyte solutions of 0.1 mol/l KNO_3 at various pH values; this was done by measuring the base currents of the rotated PbO_2 and MnO_2 electrodes. Furthermore, the use of these oxide electrodes for the determination of EDTA and other complexanes was examined.

Experimental

Chemicals. The chemicals used were of an analytical reagent grade. The supporting electrolyte solution used mainly was a 0.1 mol/l concentration of potassium nitrate. Since the oxide electrodes were sensitive to the anion components of most buffer solutions,[5,8)] the pH of the electrolyte solution was adjusted with 0.1 mol/l nitric acid and potassium hydroxide. The variation in pH value of the solution before and after the voltammetric measurements was ±0.0039 in the pH range from near 2 to 11.[10)] The nitrilotriacetic acid (NTA), ethylenediaminetetraacetic acid (EDTA), and diethylenetriaminepentaacetic acid (DTPA) were used without further purification. Redistilled water was used throughout this investigation.

Preparation of the Oxide Electrodes. The rotated lead dioxide (PbO_2) electrode was prepared by the electrolytic oxidation of 1.0 mol/l lead nitrate[8)] on a platinum disk microelectrode (0.046 cm^2) at 30±2 °C, rotated with a synchronous motor at a rate of 600 min^{-1}. Similarly, the rotated manganese dioxide (MnO_2) electrode was prepared by the electrolytic oxidation of 1.0 mol/l manganese sulfate[7)] on a platinum disk microelectrode (0.046 cm^2) in a 0.5 mol/l sulfuric-acid solution at 90±3 °C. The stationary MnO_2 electrode was prepared by the electrolytic oxidation of the same solution without being rotated.[7)] After the electrolytic oxidation of the electrode, these oxide electrodes were washed with redistilled water and used.

Apparatus and Procedures. A Yanagimoto polarograph Model P8-AP and a Princeton Applied Research Model 174A polarographic analyzer with a three-electrode system were used for the voltammetric measurements. A Corning pH-meter Model 125 was used for the pH measurements. During all the voltammetric measurements, the rotated oxide electrode was used at a rotation rate of 600 min^{-1} with a synchronous motor, Yanagimoto Model SM6S2, except for the

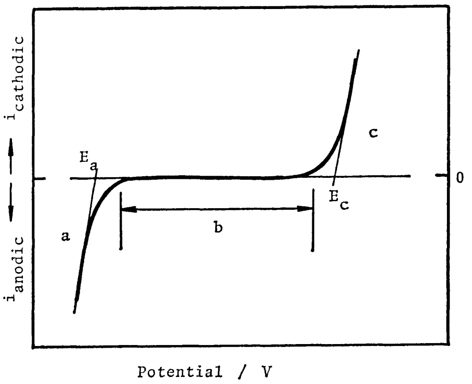

Fig. 1. Typical current-voltage curve of an indicator electrode.
a: Anodic ascending current [decomposition of medium], b: accessible potential range for an analytical application, c: cathodic ascending current [dissolution of electrode or evolution of hydrogen gas]. Ascending potential: E_a, anodic; E_c, cathodic.

investigation of the effect of the rotation rate on the redox wave. All the voltammetric measurements were carried out at a sweep rate of 5 mV/s in a thermostat of 25±0.2 °C without any deaeration of the solution. When current-voltage curves are measured at a more negative potential than zero V *vs.* SCE, the solution was deoxygenated by bubbling nitrogen gas. A saturated calomel reference electrode (SCE) and a platinum counter electrode were used.

Measurements of the Ascending Potential. Figure 1 shows a typical current-voltage curve of an indicator electrode; the anodic ascending current corresponds to a decomposition of the medium, while the cathodic one corresponds to a dissolution of the electrode or an evolution of hydrogen. The ascending potential was measured in the following way (see Fig. 1): the current-voltage curves of the rotated oxide electrode were recorded starting from +0.50 V both anodically and cathodically, and the ascending potential has defined as the potential of the point at which the tangent to the ascending curve of about 300 μA intersects with the tangent to the residual curve.

Results and Discussion

Accessible Potential Range. The accessible potential ranges have been studied for the assessments of the PbO_2 and MnO_2 indicator electrodes. The base currents of these rotated electrodes in 0.1 mol/l KNO_3 with various pH values are shown in Figs. 2 and 3 respectively.

The rotated PbO_2 electrode shows one cathodic wave at a pH value lower than 4 and one anodic wave at a pH value higher than 9, as is shown in Fig. 2. The anodic ascending current corresponds to oxygen evolution. The PbO_2 electrode may have the accessible potential range of +1.4 to +0.2 V in a 0.1 mol/l KNO_3 solution at pH values between 4 and 9.

On the other hand, the rotated MnO_2 electrode shows a small cathodic wave in its base current at the cathodic sweep, which corresponds to the reduction of MnO_2 to the lower manganese oxide, according to Eqs. 1 and 2. The anodic ascending current corresponds to oxygen evolution, while the cathodic ascending current corresponds to hydrogen evolution. Thus, the accessible potential range of the MnO_2 electrode was +1.2 to +0.3 V in a 0.1 mol/l KNO_3 solution at pH values between 3 and 10.

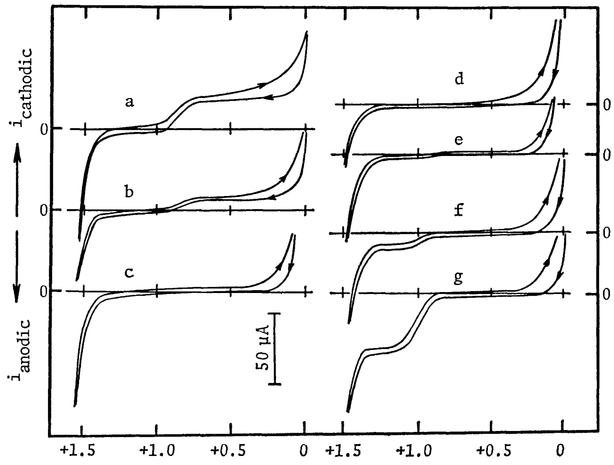

(*E vs.* SCE)/V

Fig. 2. Current-voltage curves of the PbO_2 electrode in 0.1 mol/l KNO_3 with various pH.
Sweep rate: 5 mV/s at a rotation rate of 600 min^{-1}. The pH of solution: a, 3.06; b, 3.51; c, 4.18; d, 6.14; e, 9.09; f, 9.72; g, 10.46.

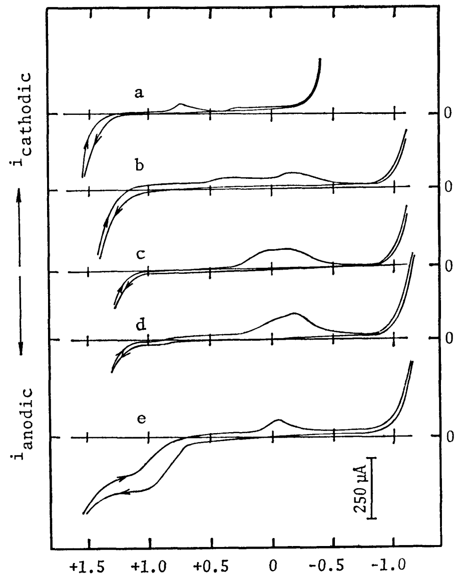

(*E vs.* SCE)/V

Fig. 3. Current-voltage curves of the MnO_2 electrode in 0.1 mol/l KNO_3 with various pH.
Sweep rate: 5 mV/s at a rotation rate of 600 min^{-1}. The pH of solution: a, 1.05; b, 3.05; c, 5.74; d, 10.11; e, 11.79.

Ascending Potentials and Self-reduction Waves of the Oxide Electrodes. In Fig. 4, the ascending potentials of the PbO_2 electrode and the half-wave potentials of the cathodic and anodic waves are plotted against the pH values. Curve a indicates the evolution potential of oxygen, while Curve b shows the ascending potential at which the PbO_2 is reduced and dissolved as Pb^{2+}, according to Eq. 3.[6] At pH values lower than 4, the cathodic wave appears and the height

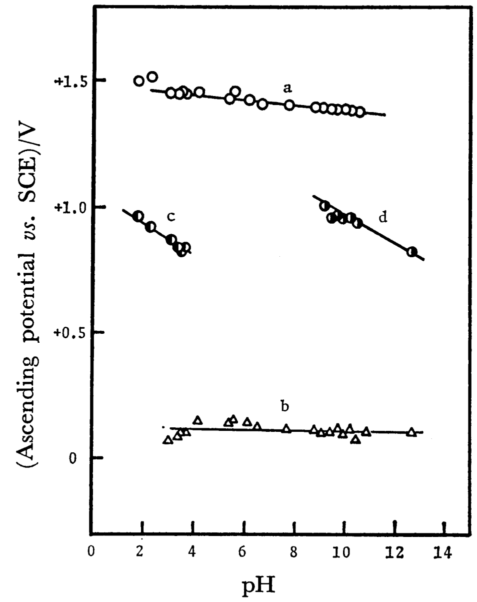

Fig. 4. Relationship between pH and wave potential of the PbO_2 electrode in 0.1 mol/l KNO_3 solution. Ascending potential: a(○), oxygen evolution; b(△), cathodic dissolution. Half-wave potential: c(◐), cathodic wave; d(◑), anodic wave.

increases with a decrease in the pH. The potential shift is −60 mV/pH (Curve c). Thus, the electrode process may be assumed to be as follows:[8)]

$$PbO_2 + H^+ + e^- = PbOOH. \qquad (4)$$

At pH values higher than 9, on the other hand, the anodic wave appears, and it increases with an increase in the pH values. Its potential is also shifted by −60 mV/pH, as is indicated by Curve d. Thus, the electrode process may be assumed to be as previously reported:[8)]

$$PbO_2 + 2H_2O + 2e^- = Pb(OH)_2 + 2OH^-. \qquad (5)$$

The ascending potential shown by Curve a is scarcely dependent on the pH of the solution. Therefore, the oxygen evolution may proceed *via* a rate-determining step, Eq. 6, as follows:

$$2PbO_2 \xrightarrow{\text{slow}} 2PbO^+ + O_2\uparrow + 2e^-, \qquad (6)$$

$$PbO^+ + H_2O \xrightarrow{\text{fast}} PbO_2 + 2H^+ + e^-. \qquad (7)$$

Curve b indicates that the cathodic dissolution of the PbO_2 may include a rate-determining step, Eq. 9, which is pH-independent, as follows:

$$PbO_2 + 2H^+ + e^- \xrightarrow{\text{fast}} PbO^+ + H_2O, \qquad (8)$$

$$PbO^+ + e^- \xrightarrow{\text{slow}} PbO. \qquad (9)$$

Similar plots are given in Fig. 5 for the rotated MnO_2 electrode. At pH values lower than 3, all the waves depend upon the pH. The ascending potential of the oxygen evolution shown by Curve a has a slope of −60 mV/pH. Thus, the following reaction may take place:

$$H_2O \longrightarrow \tfrac{1}{2}O_2\uparrow + 2H^+ + 2e^-. \qquad (10)$$

The reduction potential of the MnO_2 (Curve c′) is shifted by −120 mV/pH at pH values lower than 3.

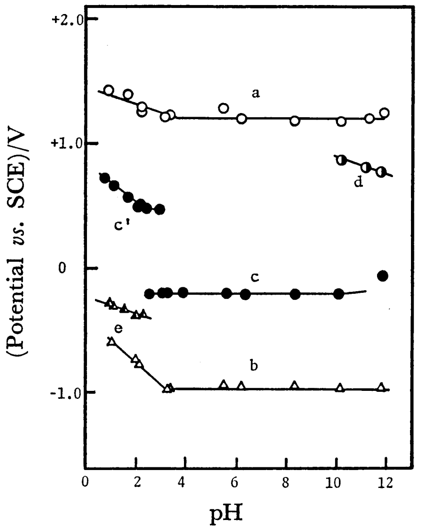

Fig. 5. Relationship between pH and wave potential of the MnO_2 electrode in 0.1 mol/l KNO_3 solution. Ascending potenital: a(○), oxygen evolution; b(△) and e(▲), hydrogen evolution. Wave potential: c and c′(●), reduction of MnO_2; d(◑), oxidation of $Mn(OH)_2$.

This result indicates that the MnO_2 on the electrode is reduced to the lower manganese state, as follows:[2)]

$$MnO_2 + 4H^+ + 2e^- \longrightarrow Mn^{2+} + 2H_2O. \qquad (11)$$

Curves e and b correspond to the evolution of hydrogen gas, and the simultaneous elution of the lower manganese state from the electrode, respectively. The wave height for Curve e decreased with an increase in the pH and disappeared at pH 3. The slopes of Curves b and e were −180 mV/pH and −60 mV/pH respectively. This phenomenon is too complicated to explain the reaction mechanism.

At pH values higher than 3, the potential of the oxygen evolution (Curve a) was pH-independent, indicating that the reaction scheme may be the same as that for the PbO_2 electrode:

$$2MnO_2 \xrightarrow{\text{slow}} 2MnO^+ + O_2\uparrow + 2e^-, \qquad (12)$$

$$MnO^+ + H_2O \xrightarrow{\text{fast}} MnO_2 + 2H^+ + e^-. \qquad (13)$$

The reduction wave of the MnO_2 appeared near −0.2 V and was pH-independent at pH values higher than 3. The same scheme as that for PbO_2 is assumed for this wave:

$$MnO_2 + 2H^+ + e^- \xrightarrow{\text{fast}} MnO^+ + H_2O, \qquad (14)$$

$$MnO^+ + e^- \xrightarrow{\text{slow}} MnO. \qquad (15)$$

The chemical species of MnO might not be eluted from the electrode, in contrast with the cathodic dissolution of the PbO_2 electrode. The evolution potential of hydrogen (Curve b) was also independent of the pH of the solution. This result indicates that the evolution may take place by means of the catalytic action of the oxide electrode and may include a rate-determining step, Eq. 17, as follows:

$$MnO + H_2O \xrightarrow{\text{fast}} Mn^+OH + OH^-, \qquad (16)$$

$$Mn^{+}OH + H_2O + e^- \xrightarrow{\text{slow}} MnO_2 + \tfrac{2}{3}H_2\uparrow, \quad (17)$$

$$MnO_2 + 3H^+ + 2e^- \xrightarrow{\text{fast}} Mn^{+}OH + H_2O. \quad (18)$$

Tafel Slope. A useful electrode for the evolution of oxygen or hydrogen is generally estimated by means of a Tafel plot ($\eta = a + b \log [i/\text{A m}^{-2}]$). In this investigation, the Tafel plot was examined for both the PbO_2 and MnO_2 electrodes from the ascending current-voltage curves of the evolution of oxygen and hydrogen. Figure 6 shows the relation between the pH and the *b* value of the Tafel slope of both the oxide electrodes. From Ref. 13, the Tafel slope (*b*) of oxygen evolution at the Pb/PbO_2 electrode is 0.12 V. In Fig. 6, Curve a indicates that the Tafel slope at the PbO_2 (Pt/PbO_2) electrode is constant, 0.08 V, against the pH of the solution. From Curve b of the MnO_2 (Pt/MnO_2) electrode, it was found that the *b* value of oxygen evolution is pH-dependent; this indicates that the electrode would be excellent in an acidic solution. Curve c displays the Tafel slope of hydrogen evolution at the MnO_2 electrode, on which the chemical species may be the lower manganese oxide. The *b* value is satisfactory for the electrode.

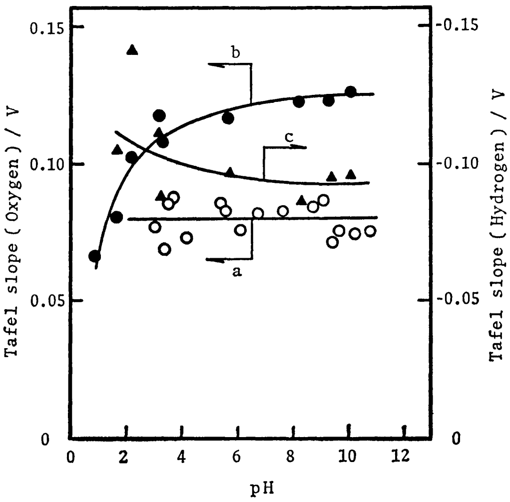

Fig. 6. Relationship between pH and Tafel slope of the evolutions of hydrogen and oxygen.
Curves: a(○), oxygen evolution at the PbO_2 electrode; b(●), oxygen evolution and c(▲), hydrogen one at the MnO_2 electrode.

Accessible Potential Ranges with Other Supporting Electrolytes. As to other systems of supporting electrolytes (constant concentration, 0.1 mol/l), each accessible potential range of both the oxide electrodes was investigated. Table 1 shows the relation between the accessible potential range at pH 5—6 and the supporting electrolyte. In each system—KNO_3, $KClO_4$, K_2SO_4, and KCl— at pH 5—6, the accessible potential range of the PbO_2 electrode was +1.4 to +0.2 V *vs.* SCE, and that of the MnO_2 electrode was +1.2 to +0.3 V, while the latter was +0.3 to −0.9 V at the lower-manganese-state electrode. The same potential ranges were obtained in the supporting electrolyte of the sodium salt instead of potassium salt.

In an acidic solution with a pH value lower than 1, the PbO_2 on the electrode was dissolved in a solution of HNO_3 and $HClO_4$, but produced insoluble films of $PbSO_4$ and $PbCl_2$ on the surface of the electrode in the solutions of H_2SO_4 and HCl respectively. This is also based upon the value of the stability constant, $\log k_1$.[14] As to the MnO_2 electrode, on the other hand, the accessible potential range was +1.4 to +0.9 V in the systems of HNO_3, $HClO_4$, and H_2SO_4, but not that of HCl (chlorine evolution).[5,7] In a basic solution, each oxide on the electrode might change to a hydroxide: $Pb(OH)_2$[8] or $Mn(OH)_2$.[5] Thus, these oxide electrodes cannot be used as dioxide electrodes, but they can be used as hydroxide electrodes.

When a buffer solution of an acetic system was used as the supporting electrolyte instead of an unbuffered solution such as KNO_3, both the oxide electrodes showed the redox waves, in spite of the small values of the stability constant,[14] as is tabulated in Table 1. Furthermore, other general buffer solutions (0.1 mol/l potassium dihydrogen phosphate, 0.1 mol/l potassium hydrogen phthalate, 0.1 mol/l potassium dihydrogen citrate, Gomori's buffer, *etc.*) were used. Similarly, both the oxide electrodes showed redox

TABLE 1. ACCESSIBLE POTENTIAL RANGE OF THE ROTATED PbO_2 AND MnO_2 ELECTRODES IN SEVERAL SUPPORTING ELECTROLYTE SOLUTIONS AT pH 5—6

Supporting electrolyte	PbO_2 electrode		MnO_2 electrode	
	$\log k_1$[a]	Accessible potential/V[b]	$\log k_1$[a]	Accessible potential/V[b]
KNO_3	0.3	+1.4—+0.2[c]	0.46	+1.2—+0.3[d] ——0.9[e]
$KClO_4$	—	+1.4—+0.2	—	+1.2—+0.3 ——0.9
K_2SO_4	2.4	+1.4—+0.2	2.14	+1.2—+0.3 ——0.9
KCl	1.32	+1.4—+0.2	0.1	+1.2—+0.3 ——0.9
CH_3COOK	0.85	Redox wave	0.80	Redox wave

a) L. G. Sillén and A. E. Martell, "Stability Constants," The Chemical Society, London (1971); Combination of the anion ligand of supporting electrolyte with the metal(II) ion. b) V *vs.* SCE. c) Dissolution of PbO_2. d) Reduction of MnO_2. e) Evolution of hydrogen.

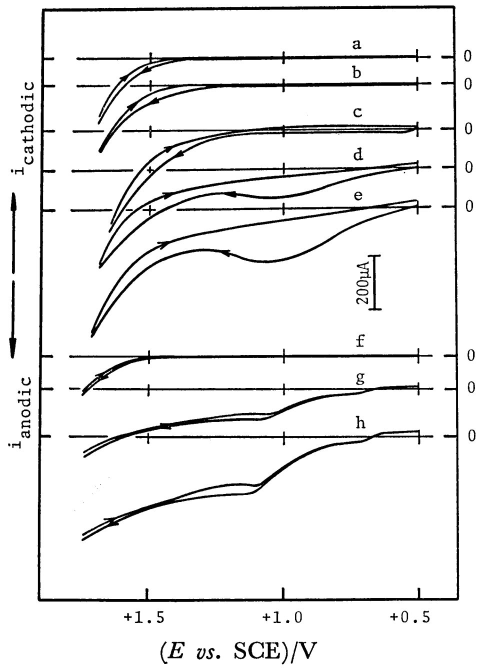

Fig. 7. Current-voltage curves of the Pt, MnO_2 and PbO_2 electrodes in 0.1 mol/l KNO_3 solution (pH 5.9) with (Curves b, d, e, g, and h) and without (Curves a, c, and f) EDTA.
Pt electrode: a and b; MnO_2 electrode: c, d, and e; PbO_2 electrode: f, g, and h. Concentration of EDTA (mmol/l), 0: a, c and f; 2.0: b, d and g; 4.0: e and h. Sweep rate: 5 mV/s at a rate of 600 min^{-1}.

waves in all these buffer solutions. Thus, these buffer solutions were not used as supporting electrolytes in this work.

Electrolytic Behavior of EDTA and the Concentration Dependence. The behavior of EDTA and other complexanes at the rotated MnO_2 and PbO_2 electrodes was also investigated. Figure 7 displays the current-voltage curves at the Pt, MnO_2, and PbO_2 electrodes in a 0.1 mol/l KNO_3 solution in the absence and in the presence of EDTA. The anodic ascending potential of the Pt electrode became a little negative only, and an anodic wave of EDTA was not observed[15] (Curve b). At the MnO_2 electrode, the anodic wave at +1.0 V appeared only in the anodic sweep. At the PbO_2 electrode, however, the pre-wave at +0.67 V and the main-wave at +0.97 V were observed in both the anodic and cathodic sweeps.

The author has previously reported on the discovery of the anodic pre-wave of EDTA at the stationary PbO_2 electrode.[8] The concentration dependence of the anodic waves of EDTA at the rotated PbO_2 electrode are shown in Fig. 8. The heights of the anodic pre-wave and main-wave were directly proportional to the EDTA concentration. The half-potential of each wave was constant. These data were reproducible within about ±3% on repeated runs. From the measurement of the anodic wave height with the PbO_2 electrode, it was possible to determine the EDTA of a concentration down to 1×10^{-5} mol/l. Figure 9 shows the relations between the wave heights and the angular velocity ω ($=2\pi N$, N: rotation rate) at the

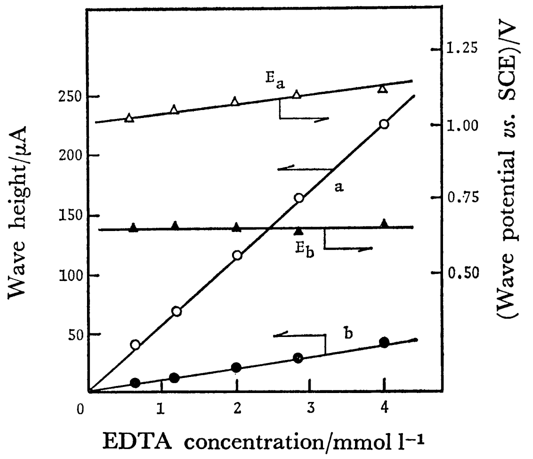

Fig. 8. Relationship between wave height, wave potential, and concentration of EDTA in 0.1 mol/l KNO_3 solution (pH 5.9).
Wave height: a(○), anodic main-wave; b(●), pre-wave. Wave potential: E_a(△), peak potential of main-wave, E_b(▲): half-wave potential of pre-wave. Electrode: PbO_2 electrode at a rate of 600 min^{-1}.

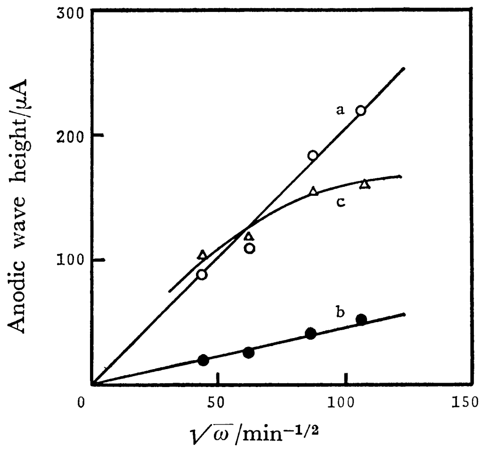

Fig. 9. Effect of angluar velocity on the anodic wave heights of 2.0 mmol/l EDTA in 0.1 mol/l KNO_3 solution (pH 6.1) with the PbO_2 (lines a and b) and MnO_2 (Curve c) electrodes.
Sweep rate: 5 mV/s. Lines a(○): PbO_2—anodic main-wave; b(●): PbO_2—pre-wave. Curve c(△): MnO_2—anodic wave.

PbO_2 and MnO_2 electrodes. A linear relationship between the wave heights and $\omega^{1/2}$ with the PbO_2 electrode was found, as is shown by Curves a and b in Fig. 9. According to Levich's opinion,[16] it follows that the limiting diffusion current, i, of the rotated disk electrode can be obtained by the use of the following equation:

$$i = \alpha\omega^{1/2}, \tag{19}$$

where α denotes the proportionality constant. It was found that the limiting currents of both the anodic waves are diffusion-controlled, because these currents were directly proportional to the $\omega^{1/2}$, Eq. 19. The anodic pre-wave is considered to be due to the adsorption of EDTA onto the electrode.[8] The anodic main-wave may be due to the complex formation of EDTA for the electrode.[8]

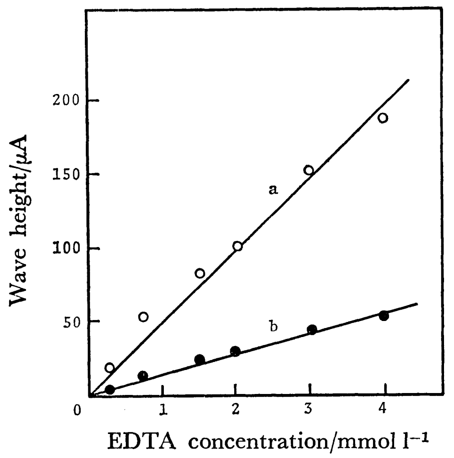

Fig.10. Relationship between wave height and concentration of EDTA in 0.1 mol/l KNO_3 solution (pH (5.9).

Lines a(○): anodic sweep; b(●): cathodic sweep. Electrode: MnO_2 electrode at a rate of 600 min^{-1}.

For the anodic limiting current of EDTA at the rotated MnO_2 electrode, a linear concentration dependence was also found passing through the point of origin, as is shown in Fig. 10. The MnO_2 electrode showed a broader anodic wave in the anodic sweep than aid of the PbO_2 electrode. In the cathodic sweep, though no well-defined anodic wave was observed, a positive current was followed (Figs. 7-d and e). The heights of the anodic wave and the positive current in Fig. 10 were measured between the anodic current at the anodic wave potential of +1.0 V and that of the base current (Figs. 7-c, d, and e). These data obtained were reproducible within about ±5% on repeated runs. From the measurement of the anodic wave height with the MnO_2 electrode, it was possible to determine the EDTA of a concentration down to 1×10^{-5} mol/l. The effect of the rotation rate of the MnO_2 electrode on the anodic wave height was also examined. In this case, however, no linear relation was found, as is shown by Curve c in Fig. 9. This finding suggests the anodic limiting current is reaction-controlled.[16] The anodic wave is considered to be due to the complex formation of EDTA for the MnO_2 electrode.

The determination of NTA and DTPA as the EDTA-type complexanes was similar to that of EDTA with the rotated PbO_2 and MnO_2 electrodes.

Comparison with Other Methods. The techniques of the determination of complexane, such as absorption spectroscopy, chelate titrimetry, and the electroanalytical method, have been described by Ueno.[17] The determining precision of each technique is not very sharp at concentrations of a complexane lower than 1×10^{-3} mol/l. A conventional electroanalytical method, such as the polarographic method and electrometric titration, is well suited for the separation and determination of complexanes, but not for trace amounts of complexane. While the present method is an electroanalytical method, it consists of the use of an anodic limiting current dependent upon the concentration of complexane, and it is as simple as a polarographic method. This method is capable of greater precision than previously reported methods,[17] and it is well suited for small amounts, 1×10^{-5} mol/l, of complexane. The PbO_2 electrode seems to be useful for determining complexane.

Behavior of the MnO_2 Electrode in an Acidic Solution. In an acidic solution, it was found that the rotated PbO_2 electrode cannot be used as an indicator electrode, since the PbO_2 shows a self-redox wave.[8] The rotated MnO_2 electrode in the acidic solution (0.1 mol/l HNO_3) has an accessible potential range of +1.4 to +0.9 V *vs.* SCE as the rotated electrode.

The electrode reaction of complexanes on the stationary MnO_2 electrode has been reported previously;[7] a characteristic cathodic current peak of manganese dioxide which increases in the presence of complexane was observed. This is because the reduction of manganese dioxide is accelerated through the complex formation. The electrode reaction is extremely dependent on the pH of the electrolysis solution. Figure 11 shows the current-voltage curves of the rotated Pt and MnO_2 electrodes in 0.1 mol/l HNO_3 containing EDTA in anodic and cathodic sweeps. When the surface of the rotated electrode was observed during this experiment, the MnO_2 was eluted and removed at +0.85 V in the cathodic sweep (Curve d) and at +1.05 V in the anodic sweep (Curve e). At these potentials, the black color of the MnO_2 material disappeared, and the white color of the base material of platinum was observed. The MnO_2 material was removed completely from the electrode after this experiment. Thus, the rotated MnO_2 electrode is considered not to be necessary for the determination of

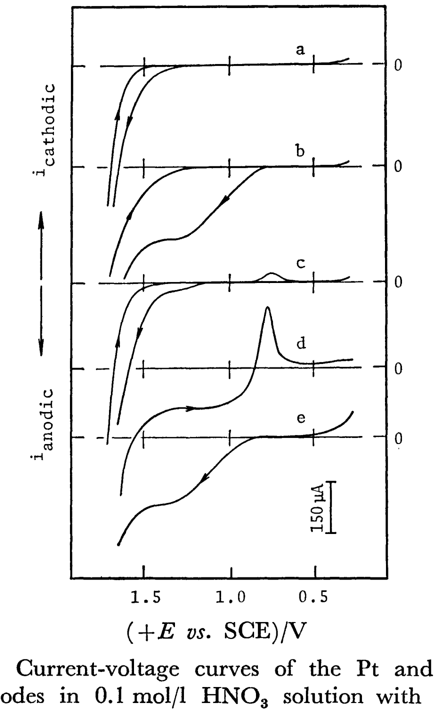

Fig.11. Current-voltage curves of the Pt and MnO_2 electrodes in 0.1 mol/l HNO_3 solution with (Curves b, d, and e) and without (Curves a and c) 1.0 mmol/l EDTA.

Pt electrode: a and b; MnO_2 electrode: c, d, and e. Surface area of both the electrodes: 0.098 cm^2. Sweep rate: 3.3 mV/s at a rate of 600 min^{-1}.

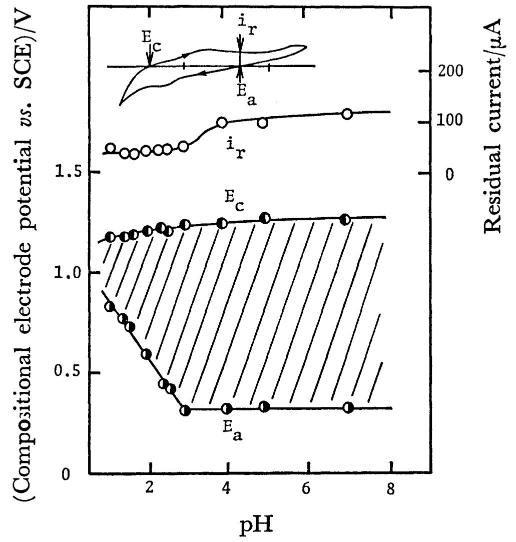

Fig.12. Effect of pH on the compositional electrode potential (zero-current level) and the residual current i_r(○) of stationary MnO_2 electrode in 0.1 mol/l KNO_3 solution with various pH.
The potential sweep range was +0.3 to +1.4 V *vs.* SCE at 30 mV/s. Compositional electrode potential: E_a(◑), anodic sweeping; E_c(◐): cathodic one. Shaded parts indicate the usable region of the stationary MnO_2 electrode as an indicator electrode.

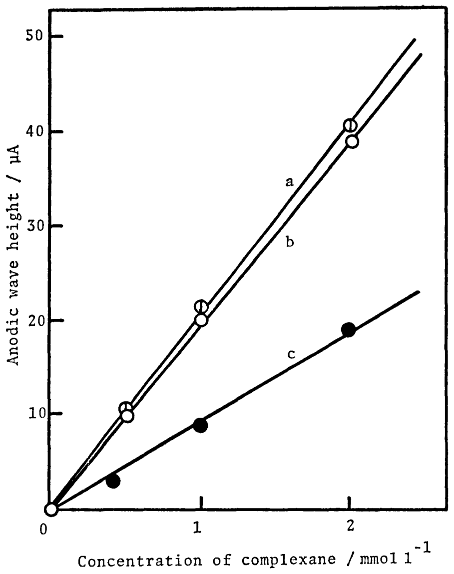

Fig.14. Relationship between concentration of complexanes and anodic wave heights in 0.1 mol/l HNO_3 solution (pH 1.5) at a sweep rate of 3.3 mV/s.
Electrode: MnO_2. Complexane: a(⦶), DTPA; b (○), EDTA; c(●), NTA. The potential at which the wave height was measured from the curve was +1.3 V *vs.* SCE.

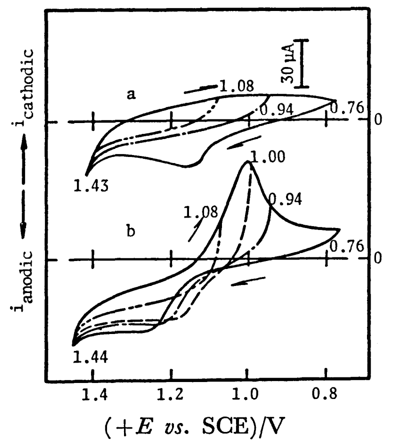

Fig.13. Cyclic current-voltage curves of stationary MnO_2 electrode with (Curve b) and without (Curve a) 1.0 mmol/l DTPA in 0.1 mol/l HNO_3 solution (pH 1.5) at a sweep rate of 3.3 mV/s.
Potentials returned in the reverse direction varied from +1.44 to +0.76 V *vs.* SCE as indicated.

complexane in an acidic solution.

According to a previous paper,[7] the stationary MnO_2 electrode is adequate as an indicator electrode for the determination of complexane in an acidic solution. The accessible potential range of the stationary MnO_2 electrode was also examined against the pH of the solution. Figure 12 shows the influence of the pH on the compositional electrode potential of the stationary MnO_2 electrode, which is defined as the potential of zero-current in the cyclic current-voltage curve (E_a and E_c). The shaded parts in Fig. 12 indicate the accessible potential range of the MnO_2 electrode in the pH region of solution. As the residual current of the MnO_2 electrode became large and the electrode became voltammetrically inert at pH values higher than 3 (Fig. 12-i_r), the stationary MnO_2 electrode is considered to be suitable for use at pH values lower than 3. In the application of the stationary MnO_2 electrode, the base current and the redox wave of DTPA in the accessible potential range are shown in Fig. 13. When current-voltage curves are measured over the accessible potential range, the electrolytic process of the anodic wave is complicated. In order to study the concentration-dependence of each complexane (DTPA, EDTA, and NTA), the height of the anodic wave was measured at +1.3 from the abscissa of the zero-current level. Figure 14 shows the relation between the wave heights and the concentrations of DTPA, EDTA, and NTA in a 0.1 mol/l HNO_3 solution. Each height was directly proportional to the concentration of complexane. These data were reproducible within about ±5% on repeated runs. From the measurement of the anodic wave-height of complexane with the stationary MnO_2 electrode, it was possible to determine the quantities of complexane in concentrations down to 1×10^{-4} mol/l.

The author wishes to express his thanks to Professor Taitiro Fujinaga and Doctor Satoshi Okazaki of Kyoto University, and Professor Kazunori Takaoka of Fukui Technical College for their valuable advice and discussions throughout this work.

References

1) I. M. Kolthoff and N. Tanaka, *Anal. Chem.*, **26**, 632 (1954).

2) M. Sato, K. Matsuki, and Y. Sugawara, *Kogyo Kagaku Zasshi*, **71**, 484 (1968); **74**, 872 (1971).

3) J. Reynaud, *Bull. Soc. Chim. Fr.*, **1968**, 4769.

4) J. A. Lee, W. C. Maskell, and F. L. Tye, *J. Electroanal. Chem.*, **79**, 79 (1977).

5) T. Yoshimura, *Res. Rep. Fukui Tech. Coll.*, *Natural Science*, **14**, 149 (1980).

6) J. P. Carr and N. A. Hampson, *Chem. Rev.*, **72**, 679 (1972).

7) T. Yoshimura, *Nippon Kagaku Kaishi*, **1981**, 240; T. Fujinaga and T. Yoshimura, *Chem. Lett.*, **1980**, 865.

8) T. Yoshimura, *Fresenius' Z. Anal. Chem.*, **307**, 197 (1981); T. Fujinaga and T. Yoshimura, *Chem. Lett.*, **1980**, 895.

9) T. Fujinaga and T. Yoshimura, *Fresenius' Z. Anal. Chem.*, **306**, 20 (1981).

10) T. Yoshimura, *Fresenius' Z. Anal. Chem.*, **308**, 445 (1981).

11) T. Yoshimura, *Fresenius' Z. Anal. Chem.*, **307**, 378 (1981).

12) T. Yoshimura, *Nippon Kagaku Kaishi*, **1981**, 307.

13) D. J. Pickett, "Electrochemical Reactor Design," Elsevier, Amsterdam (1977).

14) L. G. Sillén and A. E. Martell, "Stability Constants," The Chemical Society, London (1971).

15) K. Stulík and F. Vydra, *J. Electroanal. Chem.*, **16**, 385 (1968).

16) V. G. Levich, "Physicochemical Hydrodynamics," Prentice-Hall, N. J. (1962).

17) K. Ueno, "EDTA-Chemistry of Complexane," Nankodo, Tokyo (1977), p. 231.